Meteor Radar Phase Interferometry Calibration with Aircraft Observations and ADS-B Integration

John Marino[(1)], Nicholas Rainville[(1)], James Monaco[(1)], Scott E. Palo[(1)], and Ryan Volz[(2)]

[(1)] Ann and H.J. Smead Aerospace Engineering Sciences, University of Colorado, Boulder; email: john.marino@colorado.edu.
[(2)] Haystack Observatory, Massachusetts Institute of Technology, Westford, MA; e-mail: rvolz@mit.edu.

***Abstract*—In this study, we present a method for calibrating all-sky interferometric meteor radars using aircraft seen by the radar, along with their ADS-B reported GPS locations, as calibration targets. We also present results from the calibration procedure applied to the recently established Zephyr Meteor Radar Network along Colorado's Front Range.**

I. Introduction

A meteor radar uses reflections from the ionization trails left by meteors as tracers for activity, most often wind, in the mesosphere and lower thermosphere (MLT) region of the atmosphere. Accurate knowledge of the spatial positions of individual meteors, coupled with their recorded Doppler shifts, is vital for extrapolating wind vectors.

Phase interferometry, the method used to determine the spatial coordinates of the specular reflection point of a meteor trail as observed by radar, involves comparing the measured phases generated by the reflected plane wave incident at each sensor within an interferometric antenna array. Accurate measurement of phase is challenging, as even when each sensor channel is theoretically identical, variations in electrical length, phase center, frequency dependence, and susceptibility to interference, contribute to a phase bias on each channel. A process of calibration is necessary to determine these intrinsic phase biases.

In this study, we propose a calibration method using aircraft observed by the radar, in conjunction with aircraft positional data acquired from Automatic Dependent Surveillance–Broadcast (ADS-B) as an established reference. We will briefly outline the principles of phase interferometry, elaborate on the concept of using aircraft as calibration sources, and then present the results of applying this calibration approach to the recently established Colorado Zephyr Meteor Radar Network [1].

II. Interferometry for Direction Finding[1]

In a simple two-element phase interferometer, receiving antennas are separated by a distance, B_λ, in wavelengths. An incoming plane wave impinges on one antenna, and then the other. The extra distance the phase front has to travel to reach the second antenna is the geometric projection of the baseline vector between antennas, $\bar{B}$, onto the vector direction of the source of the plane wave, $\hat{k}$: $\Delta D = \bar{B} \cdot \hat{k}$. That distance can be represented an electrical length, or phase, φ, by multiplying the angular wavenumber conversion factor of cycles per unit wavelength, $|\bar{k}| = \frac{\tau}{\lambda}$, where $\tau = 2\pi$. By noting the geometric interpretation of dot product as relating the angle between two vectors, a relationship emerges which can be solved to find the direction or angle of arrival θ,

$$\theta = \cos^{-1}\left(\frac{\varphi}{\tau B_\lambda}\right). \tag{1}$$

Extending this technique to an array of antennas for determining three dimensional angular position in azimuth and elevation results in a vector relationship between the measured phase at each sensor location $\bar{\varphi}_{meas}$, the location of each sensor in Cartesian coordinates $\bar{\bar{B}}$, the direction of the target in Cartesian coordinates $\hat{k}$, a term to capture that the true phase is some integer multiple n of what can be measured between $-\frac{1}{2}\tau$ and $+\frac{1}{2}\tau$, a term for uncorrelated Gaussian noise $\mathcal{N}$, and finally a vector of phase biases $\bar{\delta}$ at each sensor,

$$\bar{\varphi}_{meas} = \tau \bar{\bar{B}} \hat{k} + \bar{\delta} - \tau \bar{n} + \mathcal{N}. \tag{2}$$

Solving Eq. 2 for direction of arrival (DoA) $\hat{k}$, yields a relationship with two unknown quantities: the DoA, and the vector phase biases δ,

$$\underbrace{\hat{k}}_{\substack{\text{DoA}\\ \text{Unknown}}} = \underbrace{\tau^{-1}\left(\bar{\bar{B}}^{\intercal}\bar{\bar{B}}\right)^{-1}\bar{\bar{B}}^{\intercal}}_{\substack{\text{Sensor Locations}\\ \text{Known}}} \left(\underbrace{\bar{\varphi}_{meas}}_{\substack{\text{Phase}\\ \text{Known}}} \underbrace{+\ \tau\bar{n}}_{\substack{\text{Wrapping}\\ \text{Knowable}}} \underbrace{-\ \bar{\delta}}_{\substack{\text{Bias}\\ \text{Unknown}}} \underbrace{-\ \mathcal{N}}_{\substack{\text{Noise}\\ \text{Stochastic}}}\right). \tag{3}$$

All other quantities being known[2], if the phase biases can be estimated, a solution to direction of arrival can be found. While there are several existing techniques to address the phase calibration problem, this work introduces a new method utilizing aircraft whose positions are known through ADS-B, and observed by the radar, as calibration targets.

III. Calibration with Aircraft

As of 1 Jan 2020, all aircraft flying in controlled airspace in the United States are required to be equipped with ADS-B Out avionics [3] to broadcast the aircraft's GPS-derived position, altitude, speed, and heading. These data are accessible to ground stations, nearby aircraft, and anyone with ADS-B

[1]For simplicity, we outline phase interferometry as understood from the persepective of a monostatic meteteor radar with an interferometric receiving array. While the experimental portion of the study is carried out on a forward-scatter radar with interferometric transmitting array, the equations are identical.

[2]A solution to the the phase wrapping, or ambiguity resolution, problem is described in [2]. The noise term is accommodated in a least-squares regression solution approach.

receiving equipment; providing a fortuitous opportunity for aircraft to serve as radar calibration targets.

Given the ADS-B reported location of an aircraft also visible to the radar, the phase expected to be measured by the radar for each of the antennas in the array can be determined from Eq. 2, with $\bar{\delta}$ taken to be zero, as shown in the top panel of Fig. 1. These phases are then compared to the phases recorded at each antenna, from which a set of per-antenna offsets or biases, $\bar{\delta}$, is calculated. When applied to the measured data, the resultant corrected data should match the expected data, as shown in the bottom panel of Fig. 1. In practice, since each sample recorded by the radar is a complex number with an in-phase and quadrature component, a complex correlation coefficient, $\tilde{C}$ is computed,

$$\tilde{C} = \frac{\bar{a} \cdot \bar{b}^*}{\sqrt{(\bar{a} \cdot \bar{a}^*) \cdot (\bar{b} \cdot \bar{b}^*)}}, \tag{4}$$

where $\bar{a}$ and $\bar{b}$ represent the expected and measured time series, and $*$ is the complex conjugate. The time dimension is collapsed, yielding a single correlation coefficient for the pair of time series. The resulting phase offset between time series is taken to be the vector of phase biases $\bar{\delta} = \arg(\tilde{C})$ of Eq. 2.

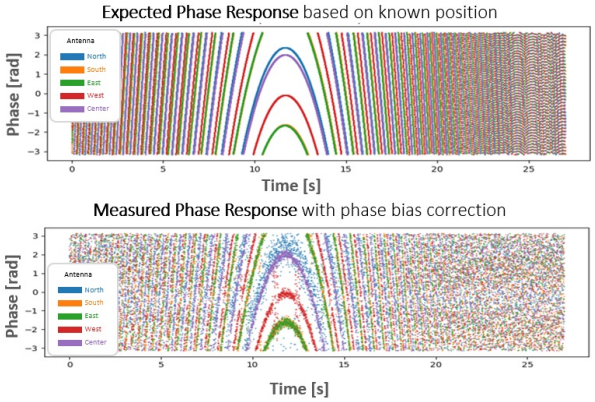

Fig. 1. (Top) Phase expected to be seen by the radar for flight UA2341 on 6 Jan 2023 based on its ADS-B reported GPS location for each sensor in the array. (Bottom) Phase recorded by the radar and corrected with $\bar{\delta}$ offsets. Note that the change in phase sense reflects the moment when the aircraft crosses over the TX-RX baseline depicted in Fig. 2.

IV. Results

The procedure of determining the offset between the phase expected to be seen by the radar based on ADS-B reported GPS location and the phase actually recorded by the radar was carried out on about 25 aircraft,

$$\bar{\delta} = \arg(\tilde{C}) = \bar{\varphi}_{model} - \bar{\varphi}_{radar}. \tag{5}$$

In practice, the $\bar{\delta}$ minimizing Eq. 5 in a least-squares sense over the ensemble of aircraft measurements was taken to be the phase bias vector utilized in Eq. 3 as the calibrated direction of arrival equation, and providing an error metric with which to evaluate the effectiveness of the calibration.

Fig. 2. Map of the Zephyr Meteor Radar Network showing transmit and receive locations and the flight path of the aircraft signature seen in Fig. 1

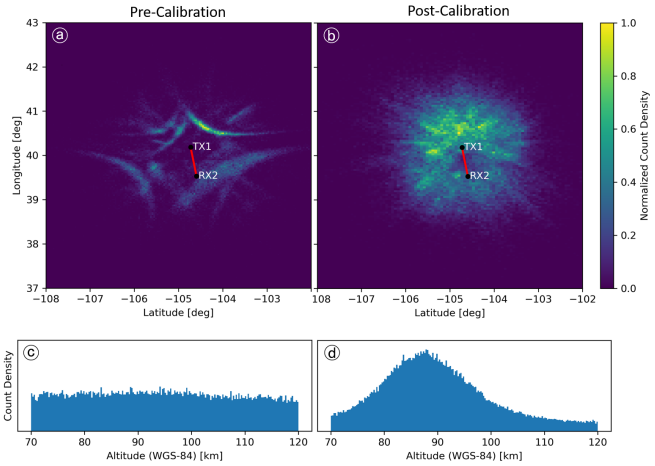

Fig. 3. Density map of echo locations calculated before ⓐ and after ⓑ calibration, along with associated height distributions ⓒ and ⓓ for the period Mar-Jun 2023 from the Platteville(TX)-Parker(RX) baseline.

Unlike the pre-calibration results (Fig. 3, left), the post-calibration computed spatial locations and height distribution of meteor echoes (Fig. 3, right) are in line with what is expected to be seen by a system operating with the frequency and geometry of the Zephyr meteor radar.

Acknowledgement

This research was supported by National Science Foundation (NSF) grant AGS-1933007 as part of the Distributed Array of Small Instruments (DASI) program (NSF-545).

References

[1] N. Rainville, J. Marino, S. E. Palo, and R. Volz, "Multistatic Radar Development for the Colorado Zephyr Meteor Radar Network" in *URSI Radio Science Letters*, 2023 vol 4.

[2] Valentic, T. A., Avery, J. P., Avery, S. K., and Livingston, R. C., "Self-survey calibration of meteor radar antenna arrays" in *IEEE Transactions on Geoscience and Remote Sensing*, 35(3):524–531.

[3] 14 CFR 91.225 in *Code of Federal Regulations*, www.ecfr.gov as of 2023.